EXPERIMENTAL STUDY ON MITIGATION OF SEISMIC RESPONSE OF A BUILDING BY VARIABLE DAMPERS

A. Ruangrassamee[1], W. Srisamai[2], and P. Lukkunaprasit[3]

1) Lecturer, Department of Civil Engineering, Chulalongkorn University, Thailand
2) Graduate Student, Department of Civil Engineering, Chulalongkorn University, Thailand
3) Professor, Department of Civil Engineering, Chulalongkorn University, Thailand
fcearr@eng.chula.ac.th, nokweerasit@hotmail.com, lpanitan@chula.ac.th

Abstract: In this study, the damping force algorithm called the viscous-plus-variable-friction damping force algorithm is proposed by combining advantageous features of typical viscous and friction dampers. The variable damper with the proposed algorithm can be represented by a viscous element placed in series with a variable-friction element. As a piston velocity increases from zero, the damping force is generated by the viscous element. This is aimed to allow energy dissipation at a small velocity. When the damping force reaches a peak value of the viscous element or a preset force limit, the sliding of the variable-friction element occurs, resulting in a constant damping force. A variable damper with the proposed damping force algorithm was developed using a magnetorheological (MR) damper. A series of cyclic loading tests of a MR damper was conducted to develop the mathematical model of the MR damper for control purpose. It is found that the proposed algorithm can be realized by the MR damper with a good accuracy. Subsequently, the MR damper was installed in the first story of a three-story steel model building. The model building is excited by a shaking table under a one-directional ground motion. It is found that the proposed damping force algorithm is effective in controlling the displacement, acceleration, and column displacement of the model building.

1. INTRODUCTION

Passive control systems have been widely applied to mitigate seismic response (Constantinou et al. 1998). Typical passive control devices are viscous dampers and friction dampers. The damping force of a viscous damper is linearly proportional to a piston velocity. The smooth change in a damping force leads to energy dissipation even when a piston velocity is small. However, a damping force is small at the end of a stroke due to a decrease in a velocity. It results in a large relative displacement of a structure in which the damper is installed. On the other hand, a friction damper provides a constant level of a damping force over an entire stroke, resulting in a large amount of energy dissipation if properly designed. However, at a slightly large damping force level, the amount of energy dissipation decreases significantly (Ruangrassamee and Kawashima 2002). And the friction damper tends to cause larger acceleration due to sudden changes of damping forces. With an emerging semi-active control technology (Spencer et al. 1997 and Sunakoda et al. 2000), the benefits of both damping force patterns can be combined. In this study, the damping force algorithm called the viscous-plus-variable-friction damping force algorithm is proposed. The variable damper with the proposed damping force algorithm was developed using a magnetorheological (MR) damper. Then, the MR damper was installed in the first story of a three-story steel model building. The model building was excited by a shaking table under a one-directional ground motion. The effectiveness of the proposed damping force algorithm in controlling the seismic response of the model building was investigated.

2. DEVELOPMENT OF VARIABLE DAMPERS

2.1 Concept of Viscous-Plus-Variable-Friction Damping Force Algorithm

The combination of viscous and friction damping force algorithms called as "viscous-plus-variable-friction (VVF) damping force algorithm" is proposed. The model representing the proposed damping force algorithm is illustrated in Fig. 1. A viscous damping element is connected in series with a variable-friction element having a variable slipping force level. As a velocity increases from zero, the viscous damping element is mobilized to dissipate energy. Once the damping force of the viscous damping element reaches its peak value in each loading direction or a force limit, the slipping force of the variable-friction element is set equal to the value, resulting in the sliding of the variable-friction element. In the reverse direction, the damping force changes in the similar manner. Fig. 2 shows the damping force vs. velocity relationship and the damping force vs. stroke relationship of the proposed damping force algorithm. The damping force algorithm is characterized by two parameters: the damping coefficient of the viscous damping element and the force limit of the variable-friction element. The force limit may represent the force capacity of a variable damper.

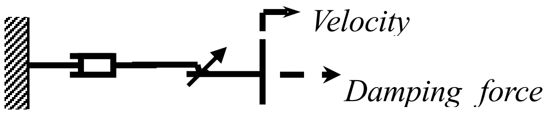

Fig. 1 Model representing the proposed damping force algorithm

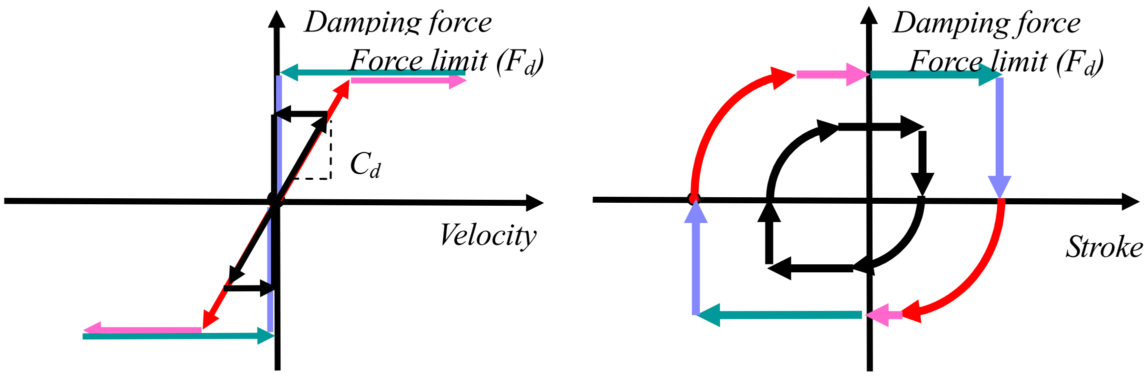

(a) Damping force vs. velocity relationship (b) Damping force vs. stroke relationship

Fig. 2 Hysteresis of the viscous-plus-variable-friction damping force algorithm

2.2 Dynamic Properties of MR Dampers

To realize the proposed damping force algorithm, a RD-1084 MR damper developed by Lord Corporation was used in this study. The damper is 237 mm long in its extended position and 197 mm long in its compressed position. So, the stroke of the damper is +/- 20 mm. The cylinder is 28 mm in diameter. The force capacity of the damper is about 60 N. The damper operates at the current of 0-400 mA. The current is supplied to the damper by a Lord RD-3002 current driver. The current driver outputs a current proportional to an input voltage in the range of about 0.5-1.5 V. In order to apply the MR damper as a semi-active control device, it is necessary to identify the damping properties of the MR damper. A series of cyclic loading tests was conducted for various loading conditions. The damping force was measured by a load cell. The load cell was connected between the reaction frame and the damper. The displacement was measured by a laser displacement transducer. The current to the damper was controlled by a microcomputer. The voltage was generated by an I/O board which was installed in the computer. Then, the current driver supplied a current proportional to the voltage. A hydraulic actuator with displacement control was used to load the damper. The damper was subjected to sinusoidal excitations. The loading frequencies were 0.01, 1, 2, and 3 Hz. The loading amplitudes were 7.5 and 15 mm. The current levels were varied as 0, 100, 200, 300, and 400 mA. The force-displacement relationships of the MR damper are presented in Fig. 3. It is seen that the damping force increases as the current to the damper increases. The force-displacement relationship of the MR damper is close to that of a friction damper. It is seen that the shape of force-displacement relationship is slightly affected by the loading conditions.

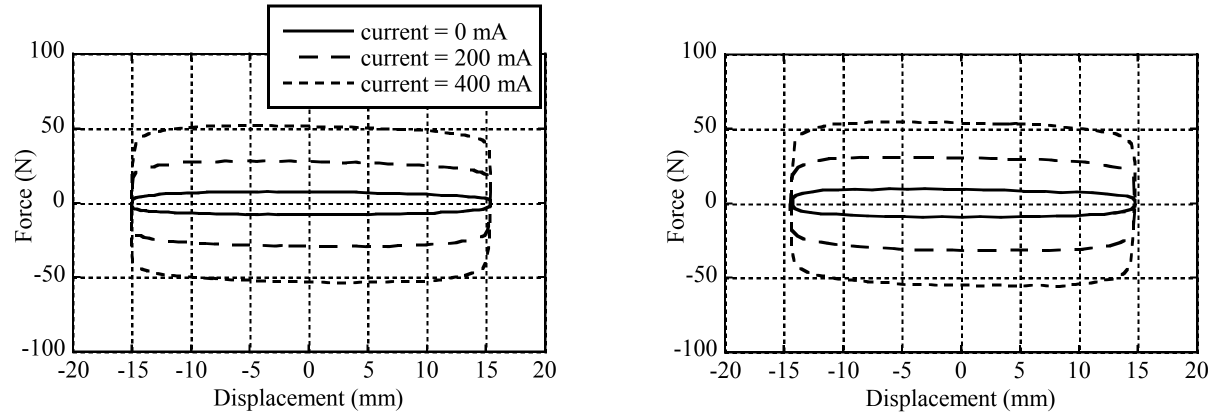

(a) Frequency = 1 Hz (b) Frequency = 2 Hz

Fig. 3 Force vs. displacement relationship of the MR damper

2.3 Control of Damping Force

To control the MR damper, the mathematical model of the MR damper is required. The MR damper was modeled from the relationship between the maximum damping force and maximum velocity as shown in Fig. 4. From a linear regression analysis, the following equation is obtained:

$$f = (3.78 + 0.123c) + (0.03 - 0.0000577c)v \quad (1)$$

where c is the current to the MR damper (mA), v is the piston velocity (mm/s), and f is the damping force (N). The current commanded to achieve a damping force can be computed from the back calculation of Eq. (1) with a known piston velocity. As it have been realized that there is a discrepancy in the damping force, a simple correction of the damping force was introduced after the back calculation. An additionally-supplied voltage (ΔV) is set as a function of the instantaneous difference between the commanded and actual (measured) damping force (Δf), as shown in Fig. 5. The effect of the slope k was investigated. Fig. 6 shows the damping force-displacement relationship of the MR damper for k = 0.04 V/N. It is found that the damping force algorithms can be realized by the MR damper with a good accuracy. For a frequency of 2 Hz, small spikes in damping forces occur after the direction of excitation is reversed. It is due to a delay in predicting the velocity of the MR damper. This may limit the application of the control algorithm for a high-frequency excitation.

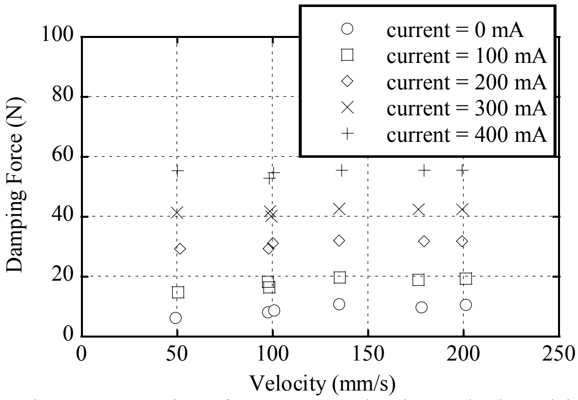

Fig. 4 Damping force vs. velocity relationship

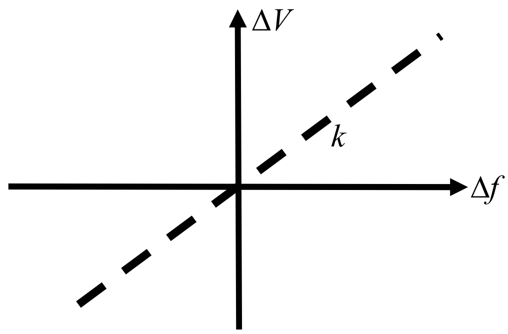

Fig. 5 Function for correcting a damping force

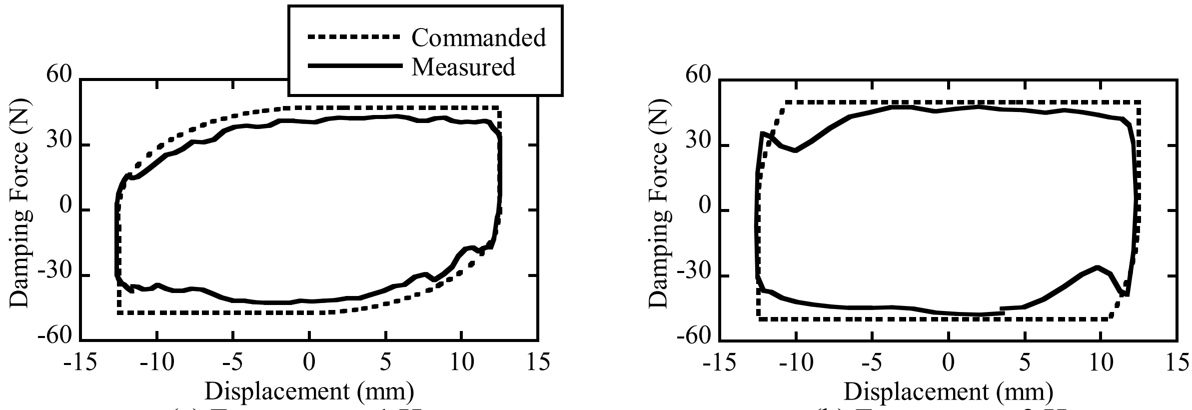

(a) Frequency = 1 Hz (b) Frequency = 2 Hz

Fig. 6 Damping force vs. displacement relationship for the VVF damping force algorithm

3. SHAKING TABLE TEST OF A MODEL BUILDING

3.1 Properties of Model Building

To investigate the effectiveness of the damping force algorithm, a shaking table test was conducted on a three-story steel model building. The model building was fabricated from steel plates as shown in Fig. 7. The masses of the 1st, 2nd, and 3rd floors are 37.5 kg, 37.4 kg, and 30.6 kg, respectively. There are four columns in each story connected to the floors by steel angles. The height of the model building is approximately 1 m. The floor size is 0.8 m by 0.4 m. From a free vibration test, the natural periods of the 1st, 2nd, and 3rd modes are 0.73, 0.25, and 0.17 s, respectively. The model building was designed to have a fundamental natural period within a typical period range of three-story steel buildings. The displacement of each floor was measured by a displacement transducer and the acceleration of each floor was measured by an accelerometer.

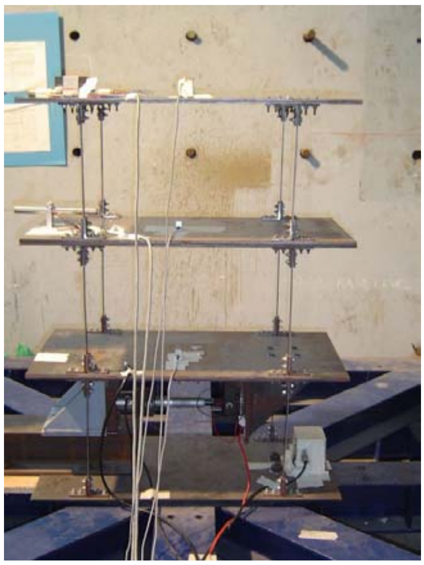
Fig. 7 Setup of shaking table test

3.2 Cases of Shaking Table Test

The model building was constructed on a shaking table and was excited by a ground motion in the long direction of the model building. The El Centro record was used in the test. The ground motion was recorded at the Imperial Valley Irrigation District substation in El Centro, California, during the M7.1 Imperial Valley, California earthquake of May 18, 1940. The peak ground acceleration is 0.35 g. The intensity of the ground motion record in the test is about 40% of the original ground motion record. The time scale of the ground motion is equal to one. It is interesting to investigate the response of the variable damper under a realistic excitation frequency. The damping force algorithm was varied as listed in Table 1.

Table 1 Cases of shaking table test

Case	Damping force algorithm	Parameters of damping force algorithm
1	No damper	No MR damper was installed.
2	No current	A MR damper was installed but there was no input current.
3	Viscous damping	Damping coefficient = 0.35 N.s/mm
4	Friction damping	Friction force = 25 N
5	VVF damping	Damping coefficient (C_d) = 0.35 N.s/mm, Friction force (F_d) = 25 N

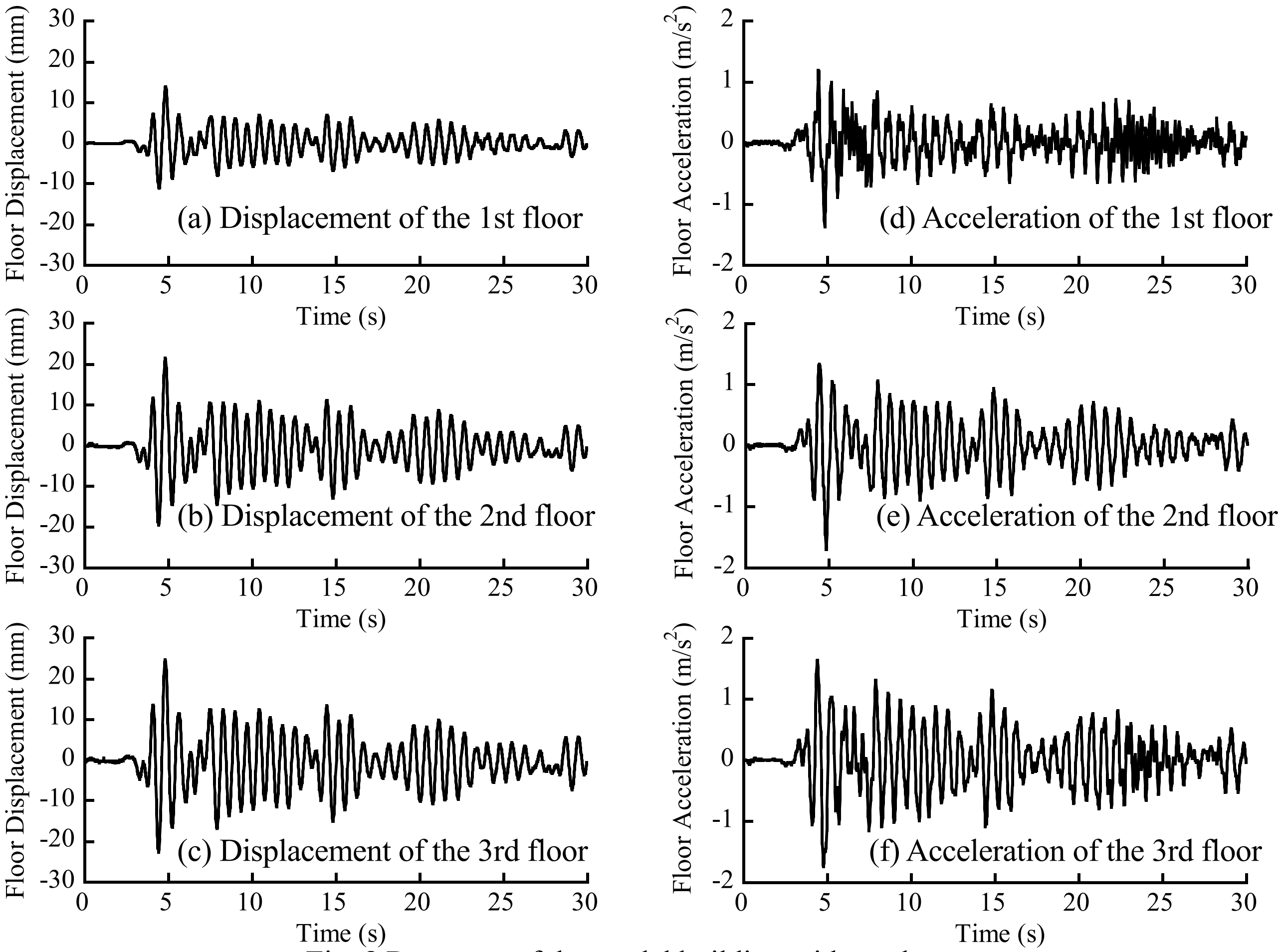

Fig. 8 Response of the model building without damper

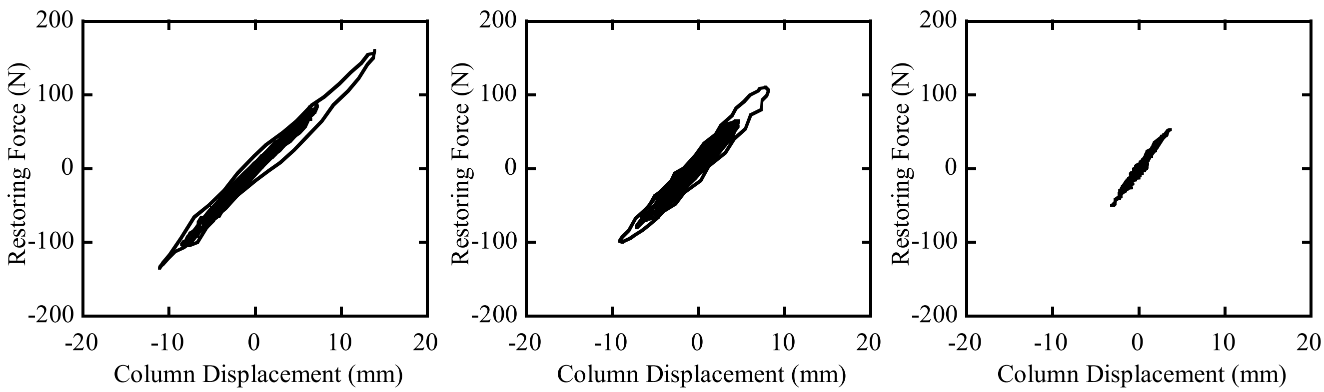

(a) The 1st story (b) The 2nd story (c) The 3rd story

Fig. 9 Restoring force vs. column displacement relationship of the model building without damper

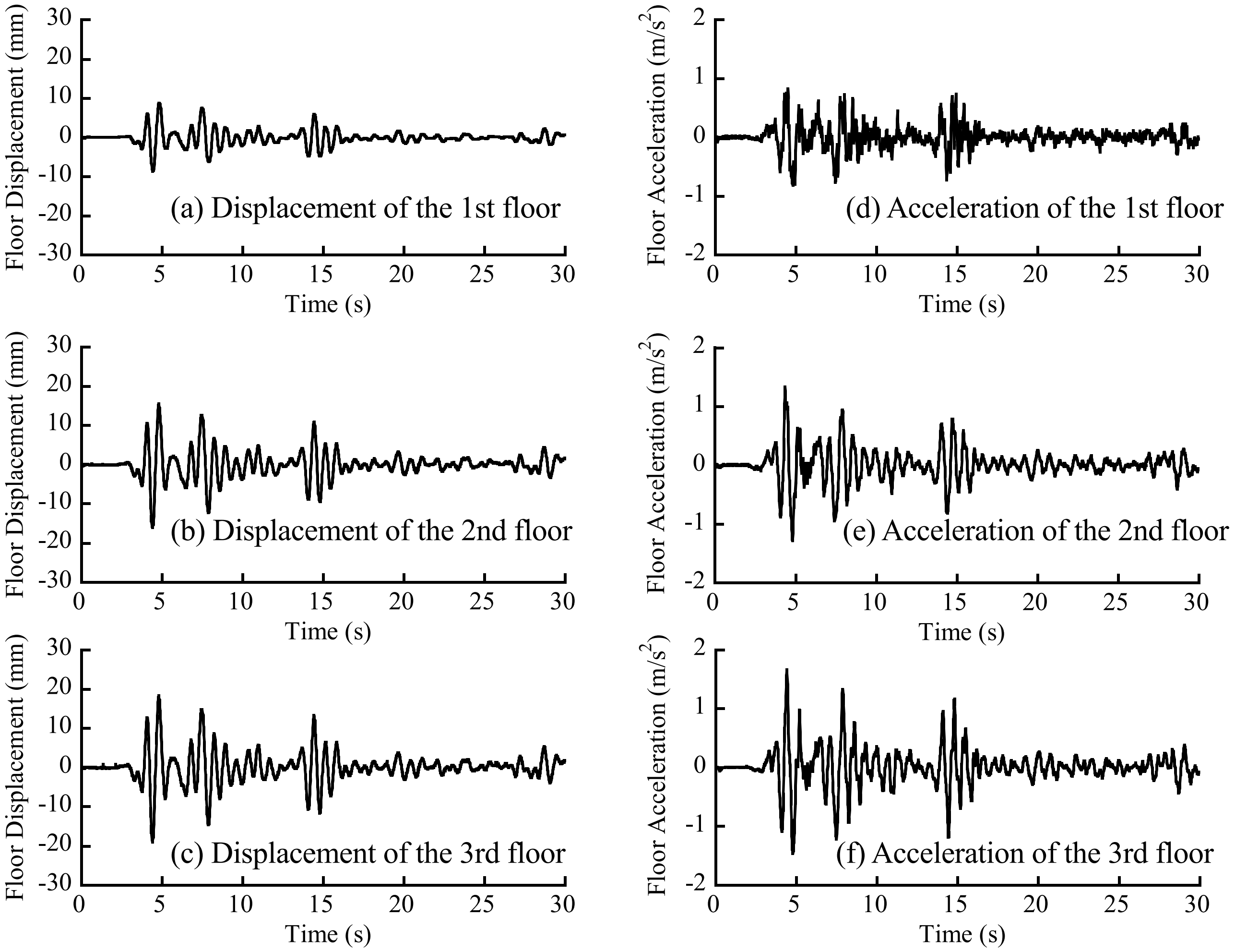

Fig. 10 Response of the model building controlled by the VVF damping force algorithm

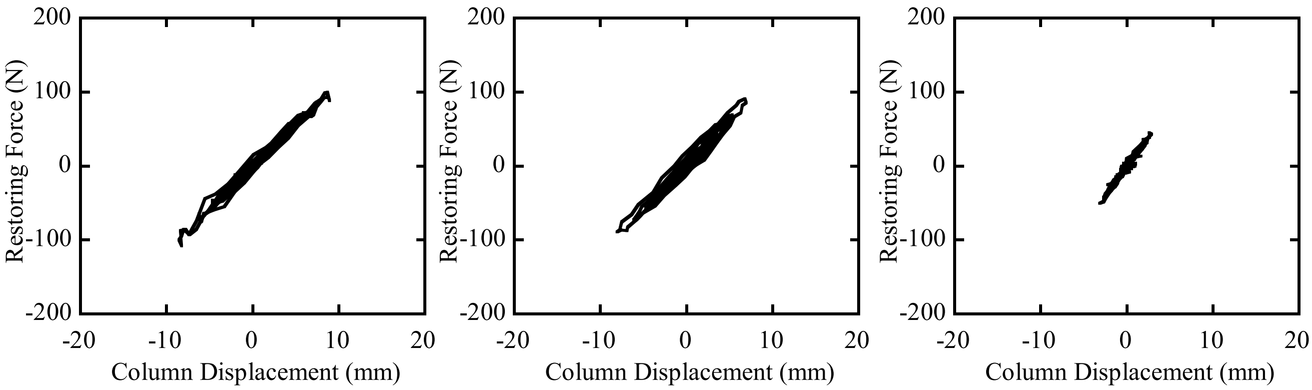

(a) The 1st story (b) The 2nd story (c) The 3rd story

Fig. 11 Restoring force vs. column displacement relationship of the model building controlled by the VVF damping force algorithm

3.3 Experimental Results

Fig. 8 shows the response of the model building without damper. The maximum displacements of the 1st, 2nd, and 3rd floors are 13.9, 21.5, and 24.6 mm, respectively. The maximum accelerations of the 1st, 2nd, and 3rd floors are 1.36, 1.69, and 1.73 m/s^2, respectively. The restoring force of columns in each story was computed from the equations of motion of a three-degree-of-freedom system with the measured acceleration and displacement. The relationship between the restoring force and column displacement in each story is shown in Fig. 9. The displacement of columns is 13.9 mm in the 1st story and varies to 3.7 mm in the 3rd story. It is seen that slight nonlinearity occurs in the columns in the 1st and 2nd stories. Fig. 10 shows the response of the model building controlled by the VVF damping force algorithm. The maximum displacements of the 1st, 2nd, and 3rd floors are 8.9, 16.0, and 19.1 mm, respectively. The maximum accelerations of the 1st, 2nd, and 3rd floors are 0.83, 1.34, and 1.66 m/s^2, respectively. Fig. 11 shows the relationship between the restoring force and column displacement in each story. The displacements of columns are 8.9, 8.1, and 3.2 mm in the 1st, 2nd, and 3rd stories, respectively. It corresponds to the percentage of reduction of 36.0%, 12.0%, and 13.5%, respectively. It is obvious that the nonlinearity is less than the case without damper. Fig. 12 shows the damping force vs. stroke relationship and the damping force vs. velocity relationship. It is seen that the damping force can be controlled with a good accuracy. For comparison, the maximum response of all cases is summarized in Table 2. The friction damping force algorithm results in more reduction of floor displacements but it causes larger accelerations. It is important to note that the maximum damping force of the friction damping force algorithm is larger than the commanded value of 25 N due to the delay in predicting the velocity as mentioned. It is seen that the VVF damping force algorithm provides slightly more reduction of displacements than the viscous damping force algorithm while yields more reduction of accelerations of the 1st and 2nd floors than other damping force algorithms. The VVF damping force algorithm is effective in controlling the response of the model building.

Table 2 Summary of experimental results

Case	**Damping force algorithm**	**Maximum acceleration of each floor (m/s^2)**			**Maximum displacement of each floor (mm)**			**Maximum column displacement of each story (mm)**			**Maximum damping force (N)**
		1st	**2nd**	**3rd**	**1st**	**2nd**	**3rd**	**1st**	**2nd**	**3rd**	
1	No damper	1.36	1.69	1.73	13.9	21.5	24.6	13.9	9.2	3.7	-
2	No current	1.00	1.47	1.61	12.3	19.8	22.9	12.3	8.2	3.2	7.5
3	Viscous	1.04	1.37	1.70	9.8	16.1	19.4	9.8	7.9	3.4	27.9
4	Friction	1.37	1.59	1.57	6.9	13.0	15.0	6.9	6.6	3.5	41.4
5	VVF	0.83	1.34	1.66	8.9	16.0	19.1	8.9	8.1	3.2	26.5

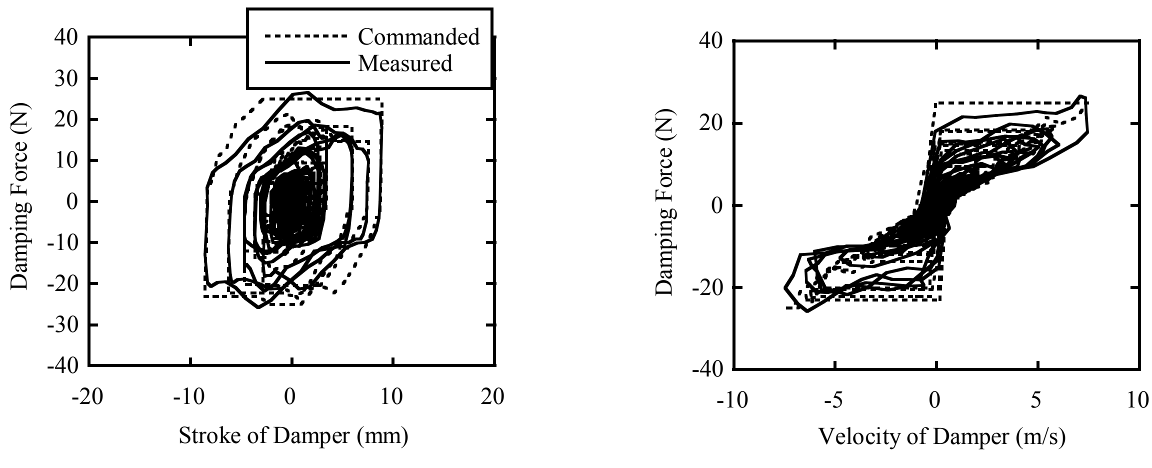

(a) Damping force vs. stroke relationship (b) Damping force vs. velocity relationship

Fig. 12 Hysteresis of the VVF damping force algorithm from the shaking table test

4. CONCLUSIONS

In this study, the damping force algorithm called the viscous-plus-variable-friction (VVF) damping force algorithm was proposed. A series of cyclic loading tests of a MR damper was conducted to develop the mathematical model of the MR damper for control purpose. It is found that the proposed damping force algorithm can be realized by the MR damper with a good accuracy. Then, the MR damper was installed in the first story of a three-story steel model building for the shaking table test. It is found that the VVF damping force algorithm provides slightly more reduction of displacements than the viscous damping force algorithm while yields more reduction of accelerations of the 1st and 2nd floors than viscous and friction damping force algorithms. The nonlinearity of columns can be reduced by the VVF damping force algorithm. The VVF damping force algorithm is effective in controlling the response of the model building. The issue related to the application of MR dampers for high-frequency excitations was noted.

Acknowledgements:

The authors acknowledge the financial support from the Thailand Research Fund (TRF).

References:

Constantinou, M. C., Soong, T. T., and Dargush, G. F. (1998), "Passive Energy Dissipation System for Structural Design and Retrofit." *Technical Report of Multidisciplinary Center for Earthquake Engineering Research*., SUNY, Buffalo, New York, USA.

Ruangrassamee, A. and Kawashima, K. (2002), "Seismic Response Control of a Benchmark Cable-Stayed Bridge by Variable Dampers." *Proceedings of the American Control Conference,* Anchorage, Alaska, USA.

Spencer, B. F., Jr., Dyke, S. J., Sain, M. K., and Carlson, J. D. (1997), "Phenomenological Model of a Magnetorheological Damper." *Journal of Engineering Mechanics*, American Society of Civil Engineers, **123**(3), 230-238.

Sunakoda, K., Sodeyama, H., Iwata, N., Fujitani, H., and Soda, S. (2000), "Dynamic Characteristics of Magneto-Rheological Fluid Damper." *Proceedings of SPIE 7th Annual International Symposium on Smart Structures and Materials*. Newport Beach, USA.